

# Fuzzy soil quality index using resistivity and induced polarization for contamination assessment in a lead and zinc drainage irrigation field study



Hamid Sarkheil <sup>a,b,\*</sup>, Khadijeh Sadoughi Noughabi <sup>c</sup>, Yousef Azimi <sup>d</sup>, Shahrokh Rahbari <sup>c,e</sup>

<sup>a</sup> Department of Applied Geology, Faculty of Earth Sciences, Kharazmi University, Tehran, Iran

<sup>b</sup> School of Mining, College of Engineering, University of Tehran, Tehran, Iran

<sup>c</sup> College of Environment, Department of Environment, Karaj, Iran

<sup>d</sup> Research Group of Environmental Engineering and Pollution Monitoring, Research Center for Environment and Sustainable Development, Department of Environment, Tehran, Iran

<sup>e</sup> Process Design Group, Chemical Engineering Faculty, Tarbiat Modares University TMU, Tehran, Iran

## ARTICLE INFO

### Keywords:

Soil contamination  
Drainage  
Resistivity  
Chargeability  
Irrigation

## ABSTRACT

Soil pollution is a significant environmental threat that cannot be directly measured from the surface. Therefore, it is essential to have metrics for assessing soil's environmental quality efficiently. The Fuzzy Soil Quality Index (FSQI) is constructed by analyzing resistivity and chargeability using four Gaussian membership functions to achieve an FSQI ranging from 0 to 100, where 0 denotes the lowest quality, and 100 denotes the highest quality. SigmaSQI and PiSQI are also introduced and statistically analyzed to enhance the performance of FSQI. Cross-validations indicate good fits, and the results are justified by experimental data. By changing the resistivity due to contaminants in the soil, the presence or absence of contamination can be traced. To achieve this, two geophysical profiles with a surveying length of 50 m on a track were performed time-lapse, once after olive and grape shrubs were irrigated with lead and zinc drainage and then again after two weeks. The contamination spread vertically and laterally so that the lateral resistivity of less than 18 Ωm reached more than 371 Ωm after the spread of pollution. As time went by, the contaminated area is reduced due to the absorption of pollutants by plant roots and microorganisms in the soil. The research results demonstrate that plants have high efficiency in absorbing pollutants due to their broad-rooted system and can reduce the risk of leaching and the movement of heavy metal contaminants to groundwater resources. Finally, to validate the presented models, five soil samples in different depths related to the presence of pollutants in the interpreted models were collected, these samples were analyzed in critical sections, and the results presented by the introduced methods showed good compliance.

## 1. Introduction

Soil is a crucial natural resource that supports 95% of human food preparation, and its health is necessary for food security and sustaining life of Earth (Sarkheil et al., 2020). Soil pollution is a significant threat to the ecosystem and is caused by direct disposal of pollutants or indirect leaching of wastewater and effluents (Kuras et al., 2016; Huang et al., 2019). Contaminants transferred to the soil can contaminate groundwater, leading to irreparable environmental damage (Sarkheil et al., 2014; Zeng et al., 2019). Metallic mines wastewaters and effluents are essential sources of pollutants (Maleki and Hashmati Moghadam, 2014). Soil compounds have a high but limited potential for filtering and absorbing pollutants, destroying and reducing contaminants' adverse effects. Protecting soil safety and health as the primary crop production

source and an essential basis for maintaining and sustaining human survival is a public duty for all individuals (Kabata Pendias, 2010).

Soil contamination by waste chemicals has raised environmental concerns. Heavy metals are also crucial in low concentrations due to their non-degradability and physiological effects. Heavy metals as a contaminant are transmitted through the food chain and threaten human health (Singh and Kalamdhad, 2011; Mazej et al., 2010). Due to the various levels of complexity of the soil and the different sources and characterization of influences, heavy metal pollution concentration is highly variable at different soil levels. Their distribution pattern generally has spatial heterogeneity (Maas et al., 2010). The heavy metals severely affect the soil's upper horizons, altering their chemical properties, natural structure, and biological activity (Gillet and Ponge, 2002; Dijkstra, 1998). Mine wastes or acid mine drainage (AMD)

\* Corresponding author.

E-mail address: [Sarkheil@knu.ac.ir](mailto:Sarkheil@knu.ac.ir) (H. Sarkheil).

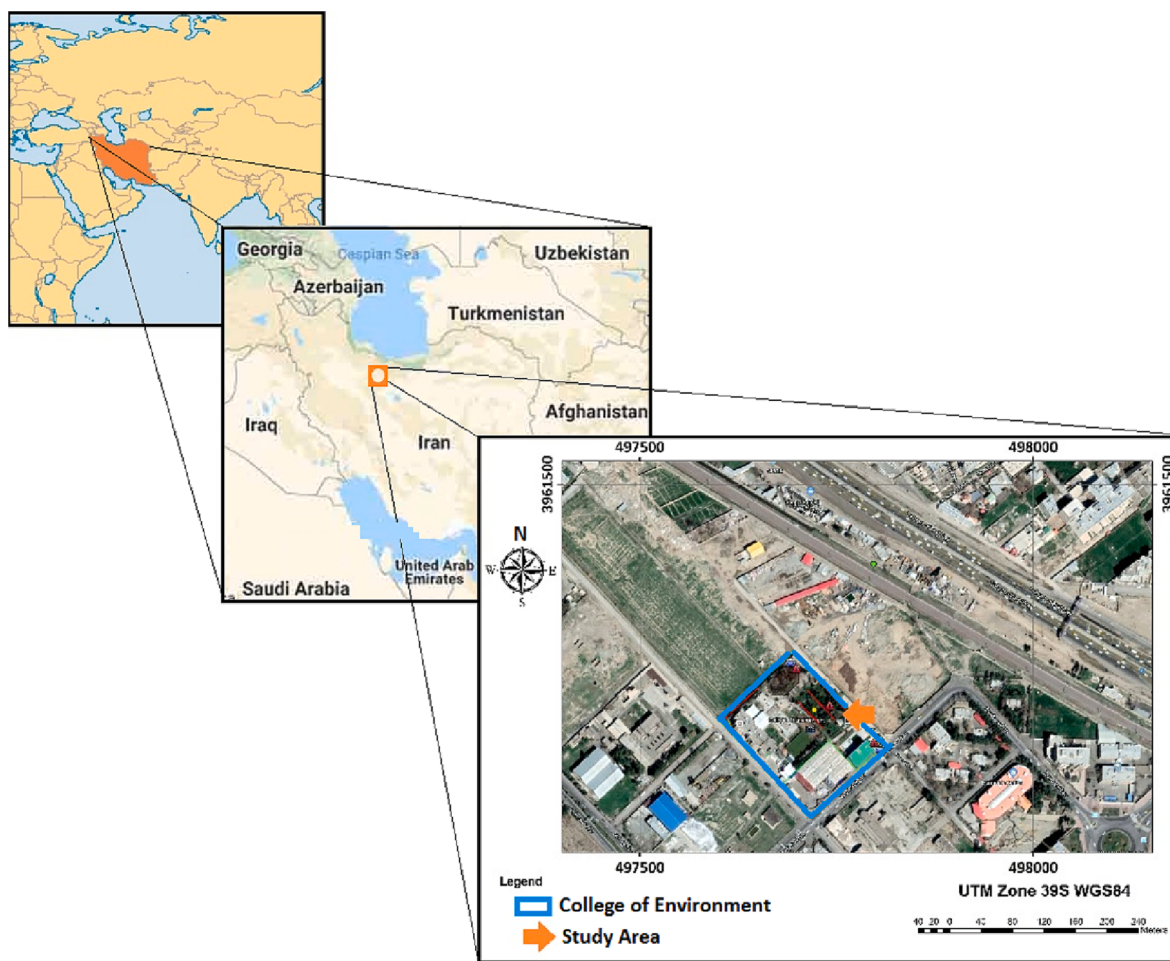


**Fig. 1.** The geographical location of the site under investigation.

accumulation, especially leaching from tailings dams, are important sources of environmental problems in mining activities boundaries and need special attention.. Acidic mine drainages can lead to acidity and accumulation of heavy metals and metalloids (highly toxic elements such as arsenic). Sulfate in weathered zones under mineral tailings layers and entering the food chain is extremely dangerous for humans and other creatures due to its high toxicity (Maleki and Hashmati Mogqaddam, 2014). The soil's connected pores cause the pollutants to move from one place to another and be less stable to these pollutants transfer (Akowuah, 2011). The pollutants released from effluent that are not absorbed by plants' roots move down the earth and expose groundwater to pollution.

Geophysical methods, particularly geoelectric (resistivity and chargeability), are expanding to study contamination propagation. Groundwater affected by contaminated solutions has resistivity differences from its surrounding environment (Kuras et al., 2016). The primary purpose of electrical methods is to measure the earth's electrical resistivity (Magiera et al., 2019). Because mineral wastes contain acid mine drainage and heavy metals, they can cause changes in the electrical conductivity of the earth's subsurface. (Campbell and Fitterman, 2000). Geoelectrical methods, especially geoelectric (Resistivity and Chargeability) have been successfully used to detect and evaluate different soil and groundwater contamination characteristics and determine the optimal location of drilling wells for direct sampling of soil and groundwater in a contaminated zone and the plume's boundary shape in the groundwater (Moradzadeh et al., 2007). Because of most pollutants' conductive properties, electrical methods have been widely used as an indirect geophysical method for controlling environmental pollution

(Sharifi et al., 2014; Ariafar et al., 2014; Sarkheil and Habibi Rad, 2015).

This study aims to use pattern recognition to identify leakage pollution from mineral tailings dams and the dispersion of mine contaminant drainage into the soil in an irrigation test as an alternative method. Controlling inlet contamination using plant roots has been part of the goal.

So as an innovative method by designing irrigation experiments with lead and zinc mine effluent, this spread of pollution has been studied indirectly. Also, tree roots' effect on pollution accumulation, conduction, or stabilization has been studied with the geoelectrical analytical method, without drilling and manipulating the land and soil cover in areas. Geoelectric surveying (Induced Polarization\IP and Resistivity\RS) has been used to test the contaminated region's infiltration changed within the subsoil.

## 2. Materials and methods

The study area is in the Alborz Province, Karaj City. The eastern part of the College of Environment adjacent to the research garden, with a height of 1305 m (above sea level), the groundwater table depth in the studied area region was 150 m and longitude and latitude are 354741.03N and 5058'30.93E (Fig. 1).

Anguran lead and Zinc Processing Plant is located about 95 km away from Zanjan city, Zanjan Province. The high-grade feed contains more than 33% zinc and less than the low-grade one. The low-grade ore is screened into two size fractions, -2 mm (Size below 2 mm) and +2 mm (Size over 2 mm). The -2 mm fraction goes to the Pb flotation circuit.

**Table 1**

Sample analysis of wastewater used by tailings dam and zinc deposits of Anguran.

Concentration (ppm)	Elements
410	Lead
4300	Zinc
23,400	Nickel
21,000	Cadmium
Little	Arsenic

The tailing from the –2 mm fraction circuit containing 20–23% zinc is sent to tailing dams. According to the sampling standard, samples were taken equally from the tailings dam's four segments under internal protocols and mixed parts.

The effluent sample from the Zanjan-Anguran lead and zinc processing plant's tailings dam was used as contaminated water to irrigate olive and grape trees. Lead and zinc wastewater samples of 100 L volume were analyzed by induced coupled plasma optical emission spectrometry (ICP-OES), and the results are shown in Table 1.

This study employs the geoelectric method to investigate the variations in soil resistivity and chargeability properties in response to contamination. 36 sampling points were measured, yielding 36 sets of resistivity data and 36 sets of chargeability data. The data were collected in two stages, denoted as profile01 and profile02, with one profile surveyed twice as a Time-Lapse. The length of the profile was 550 m, with 11 electrodes placed at intervals of 5 m between every two lateral electrodes. This method helps determine underground lithology, assess groundwater depth, and assess contamination of plume extension and transportation areas. This method measures the earth layers' electrical resistivity variations using the two currents and two potential electrodes above the surface (Sarkheil and Hassani 2009; Sparrenbom Charlotte et al., 2017). The current electrodes (A, B) and potential electrodes (M, N) are generally arranged in a linear array (Fig. 2).

Geoelectrical methods are widely used in environmental and engineering investigations to evaluate the subsurface structure and properties. These methods rely on measuring the electrical resistivity or conductivity of the earth to provide information on subsurface structures and properties, including the presence of groundwater, contamination, and mineral deposits. Two important parameters in geoelectrical methods are chargeability and resistivity.

The resistivity ( $\rho$ /unit: Ohm\*meter) can be calculated from the electrical current (I) and the potential difference ( $\Delta V$ ). The apparent resistivity of the soil can be determined based on the known difference

between the electric field potential ( $\Delta V$ ) and the current (I) and the distance between the electrodes, and K is called the geometric factor (unit: meter) and can be calculated from the electrode spacing. So, soil resistivity has been measured from the surface to the depth.

Changeability refers to the change in electrical resistivity or conductivity of the subsurface materials in response to changes in the applied electrical field. This parameter is affected by several factors, including the pore fluid conductivity, mineralogy, and the presence of conductive or resistive bodies. Changeability is typically quantified by the formation (Equation (1)) factor (F), which is defined as the ratio of the bulk electrical conductivity of a material to its pore fluid conductivity (Telford et al., 1990):

$$F = \sigma_b / \sigma_f \quad (1)$$

Where  $\sigma_b$  is the bulk electrical conductivity and  $\sigma_f$  is the pore fluid conductivity.

Induced polarization (IP) is another critical parameter in geoelectrical methods. IP refers to the ability of a material to store charge in response to a changing electrical field. This effect is particularly strong in minerals with polarizable interfaces, such as clays and sulfides. IP can be quantified by the complex resistivity (Z), which is a function (Equation (2)) of both the resistivity ( $\rho$ ) and the phase angle ( $\theta$ ) between the electrical field and the induced polarization (Kemna, 2012):

$$Z = \rho(1 + i\tau) \quad (2)$$

Where  $i$  is the imaginary unit and  $\tau$  is the time constant, which is related to the polarization relaxation time.

Both chargeability and resistivity can provide valuable information on subsurface structures and properties. This study was based on field surveying, measurement, data processing, and inverse modeling. Field surveying and operations were carried out using Terrameter SAS 4000C of ABEM Swedish Company (Fig. 3). It is also possible to see electrode locations and the pseudo-depth from the measured network's electrode configuration.

Irrigation with the effluent of the lead and zinc processing plant was carried out in profile. Approximately 100 L of wastewater have been used for irrigation each time. One was on 24 February 2018, and measurements were taken shortly after the irrigation operation. After two weeks (on 10 March 2018), the measurements were repeated to detect contamination. Moreover, show the pattern plume of the contamination in the soil subsurface, between two measurement periods (in rainless conditions) and only with pre-designed irrigation.

Some grape and olive shrubs trees exist in the surveyed profile path with 5 to 8 m root length (Smart et al., 2006; Masmoudi Charfi et al.,

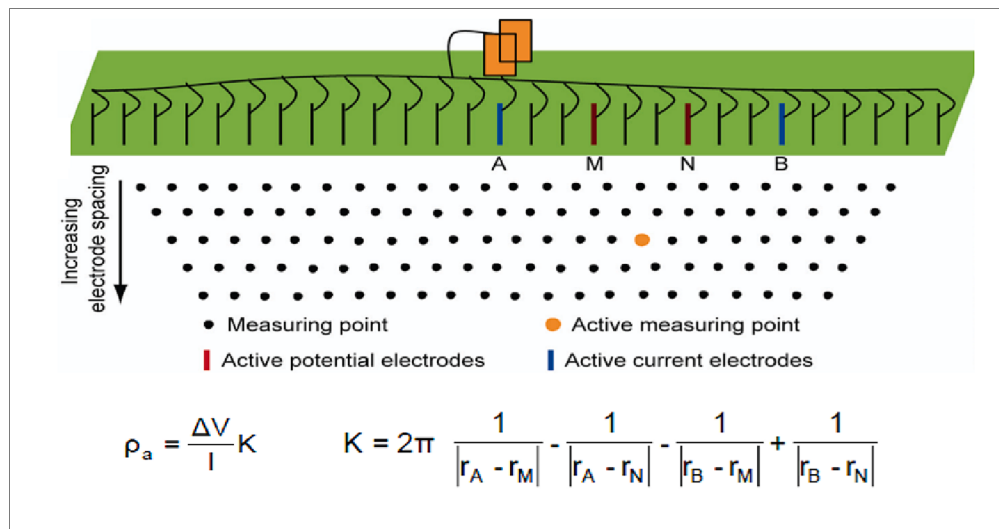


Fig. 2. Geophysical survey and relations.



**Fig. 3.** Geophysical instrument and data measurement sheet.

**Table 2**  
Distinguishment of fuzzy rules for FSQI.

Fuzzy Rule	Weight
If IP is Very Low: FSQI is Good Quality	1
If IP is Low: FSQI is Average Quality	1
If IP is High: FSQI is Contaminated	1
If IP is Very High: FSQI is Very Contaminated	1
If Resistivity is Very Low: FSQI is Very Contaminated	1
If Resistivity is Low: FSQI is Contaminated	1
If Resistivity is High: FSQI is Average Quality	1
If Resistivity is Very High: FSQI is Good Quality	1

2011). Due to the previous studies' experience similar to the data collection team, the Dipole-dipole array was used compared to other arrays. This array measured the data to penetrate deeper and investigate the contaminant dispersions/diffusions pattern. Measurement of 6 layers depends on depth from at least 4.16 m pseudo-depth to 22.4 m with a 50 cm-copper-coated steel electrode in 60 subsurface blocks. Due to electrode configuration, two-thirds of electrode length ( $\frac{2}{3}$ ) were placed in the ground to transmit more electrical current. The Terrameter SAS 4000C set was located between the current and potential electrodes, simultaneously examining the electrical current path. The induced polarization (IP) factor was surveyed three times. This operation determines resistivity and induced polarization for each rectangular subsurface block (60 blocks). It can produce a quasi-cross section of apparent resistivity and induced polarization factor. Consistent with actual measurement, 36 geoelectrical survey points were obtained from resistivity and chargeability data. The measured data were modeled by

the Least-Square inverse method of RES2D&3DINV software.

### 2.1. Fuzzy soil quality index (FSQI)

The researchers have studied fuzzy quality indices for Air Quality via Sarkheil and Rahbari, 2016; Sarkheil et al., 2018a; Fuzzy radon hazard index assessment via Sarkheil et al., 2023 and Water and Wastewater quality indices via Sarkheil et al., 2018b; Sarkheil et al., 2021 and Sarkheil et al., 2019.

In this research, a fuzzy soil quality index is constructed for the environmental assessment of soil quality. The fuzzy index is based on two factors resistivity and Induced Polarization. Furthermore, as a figure, the proposed FSQI ranges from 0 to 100 in four fuzzy MFs of Gaussian Types. All factors are categorized into four levels Very Low, Low, High, and Very High. The fuzzy rules for the prepared FSQI.fis are distinguished in Table 2.

### 2.2. Sigma soil quality index (Sigma-SQI)

To prepare classic data for validating the fuzzy attitude proposed sigma-SQI (presented in this part) along with Pi-SQI (in the next part). The primary notion comes from aggregating contamination factors of resistivity and chargeability with weighting arithmetic averages. As both factors have the same effect on contamination concentration, the weights are equal to 0.5. The main formula for Sigma-SQI is represented in the following. Sarkheil et al. 2018, Sarkheil et al. 2021, and Sarkheil et al. 2019 for water and wastewater quality indices have studied some analogous analyses. Here the notion is transformed for soil quality index

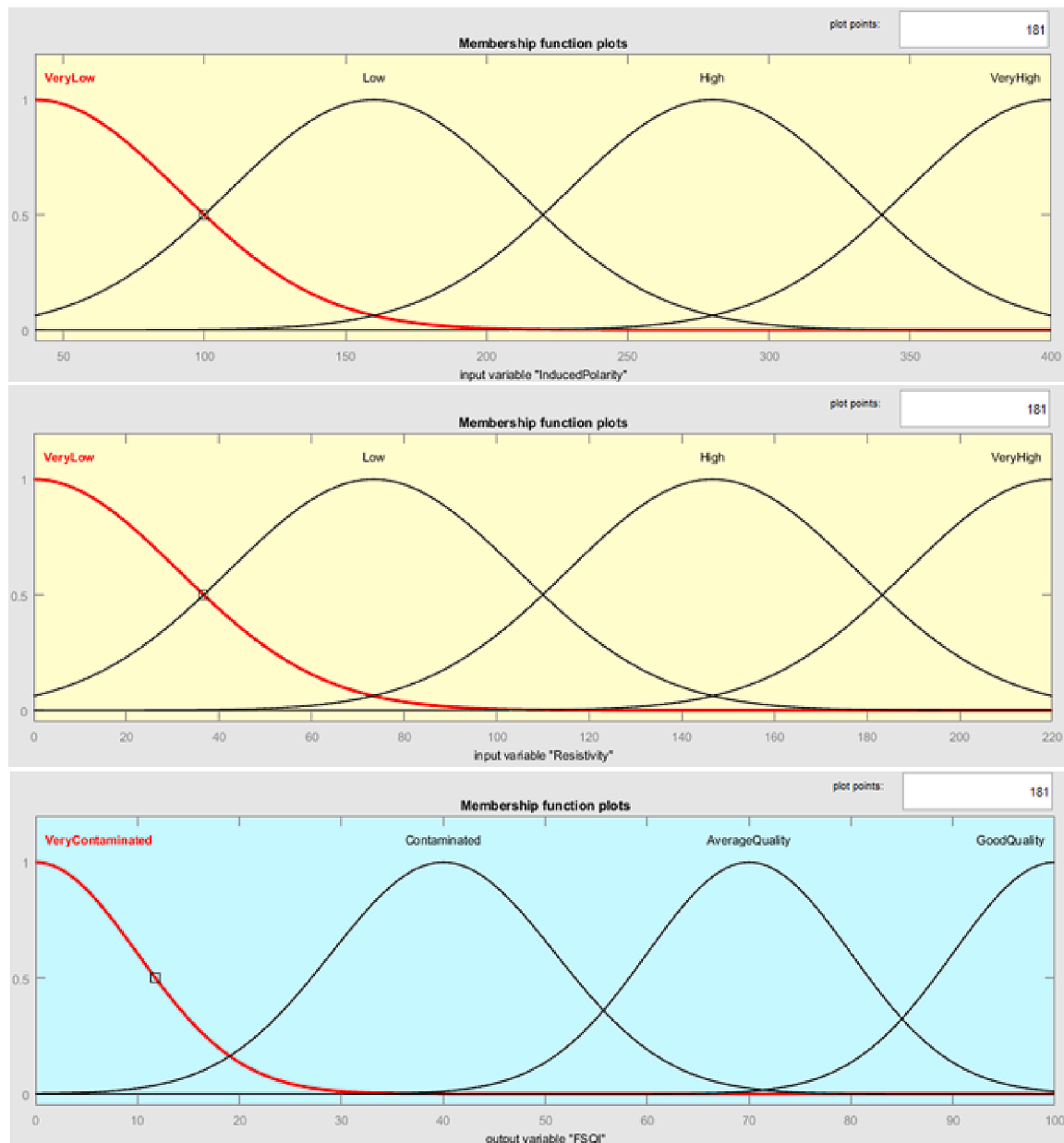


**Fig. 4.** Membership Function assignment for FSQI fuzzy inference system.

by innovation (Equation (3)).

$$\text{SigmaSQI} \equiv \sum_{i=1}^{\text{NoElements}} W_i Q_i \quad (3)$$

Where  $W_i$  and  $Q_i$  are the element i's weight and quality,  $Q_i$  is introduced for resistivity and chargeability (Equation (4) and (5)).

$$Q_R \equiv 100 \frac{(R - R_{\min})}{(R_{\max} - R_{\min})} \quad (4)$$

$$Q_{IP} \equiv 100 \frac{(IP_{\max} - IP)}{(IP_{\max} - IP_{\min})} \quad (5)$$

It is noted that the element's quality ranges from 0 for the lowest quality to 100 for the highest quality.

### 2.3. Pi soil quality index (Pi-SQI)

After proposing aggregated weighted SQI, it is proposed the multiplicative weighted SQI. The Pi-SQI is defined as Equation (6).

$$PiSQI \equiv \prod_{i=1}^{\text{NoElements}} (Q_i)^{W_i} \quad (6)$$

Where  $W_i$  are corresponding weights and  $Q_i$ s are synonymous as that with SigmaSQI.

### 3. Results and discussion

One challenge is making relationships between soil parameters against electrical resistivity. The basic assumption is that the soil structure plays an insulator (in sandy soils) while the electrical current flows through the soil's water pores and routes. If the water content is constant, the soil resistivity is related to the salt dissolved in the soil water in the ionic composition. Also, the conductivity of solutions

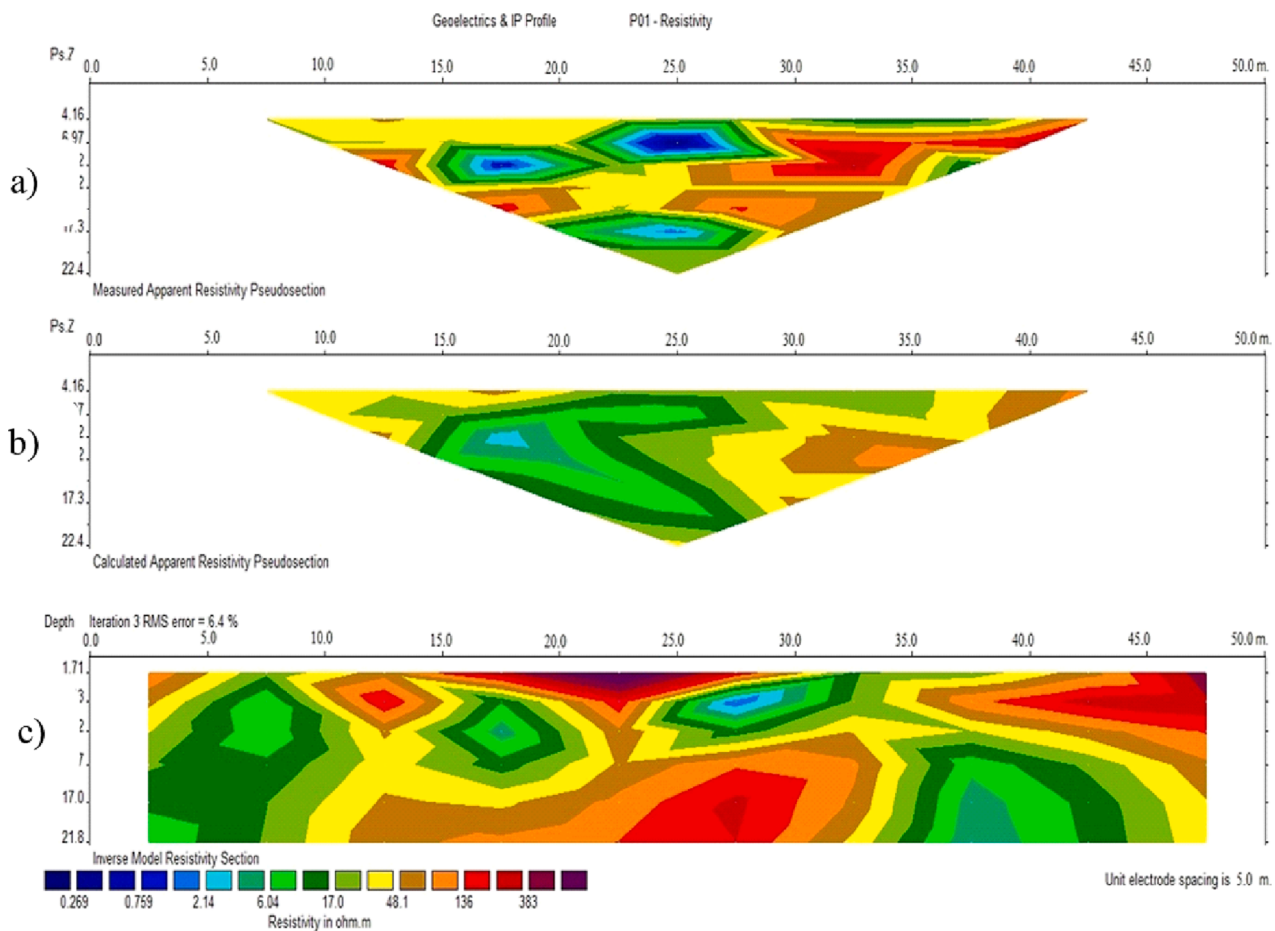


**Fig. 5.** a) Pseudo-section of measurements, b) pseudo-section of inversion, c) inverted resistivity model in profile P01 with 5 m electrode spacing.

accompanies the significant constituents (e.g., sodium cations and chloride anions).

The resistivity range was between 1.8 and 389 O.m, and Induced polarization was between 2.34 and 366 msec. During research surveying, the currency between 200 and 1000 mA was transmitted. The current cycle used is a +/0/-/0 sequence (50% duty cycle), with a 1 to the 1.1-sec pulse length. The chargeabilities were measured in 8-time windows with 100 ms fixed duration for the first instrument used and with time windows varying from 50 to 150 msec for the second one, starting 10 msec after the current turn-off. The signals were automatically corrected for variation in the background potentials via measurement of the potential before and after each measurement cycle.

There is a direct relationship between the electrical conductivity (in the range of 0.5 to 0.9 ds/m in the sample analysis) and the number of water-soluble elements and a similar correlation with other factors and water quality content. Small elemental water solubility changes affect conductivity (Jelenska et al., 2008; Knodel et al., 2005). Therefore, these factors can record water composition changes affected by groundwater pollution. When electrical conductivity is calibrated and based on an analytical evaluation, this property can be valuable information to assess soil and water environment (Loke et al., 2013; Koda, 2012).

### 3.1. Two-dimensional model results of profile 01

Resistivity and Induced polarization datasets after surveying profile 01 (Fig. 4) were inverted and modeled using RES2D&3D INV. Using the measured data (Potential difference values,  $\Delta V$ ), the electrical current intensity ( $I$ ), and considering the geometrical factor of the electrode arrangement (as a dipole-dipole array), the apparent resistivity of the

subsurface layers is calculated. Fig. 5 a, b, and c, show the measured apparent resistivity, calculated apparent resistivity, and inverse resistivity model.

#### 3.1.1. Investigation of resistivity and induced polarization of profile P01

Fig. 6 shows the shrubs' location and the resistivity levels to start irrigation. Fig. 6a shows the 2D inverted model of the resistivity (by ohms/ $\Omega$ ms), and Fig. 6b shows the 2D inverse induced polarization model (in millivolts per millisecond). The horizontal axis represents the electrode spacing (in meters) in both forms, and the vertical axis indicates pseudo-depth (in meters).

With a resistivity of less than 18 $\Omega$ m, areas affected by pollution are pale green to dark blue. The decrease in the resistivity was initially vertical; due to pollution, these depths increased over time. Lateral resistivity reductions are marked in the subsurface layers of the earth along with the profile. Lateral expansion of areas with decreasing resistivity may be due to increased irrigation water with high electrical conductivity. It moves more or less vertically in the unsaturated zone, and it is distributed after reaching the saturated zone transversely.

The most likely explanation for the lateral spread in decreased resistivity is that the lateral transport of groundwater in the soil profile is slow diffusion or mass transport of high-ionic water in the groundwater zone. The effluent was applied to the soil at once, so the rapid water movement could influence leaking and reactive transport or leaching into the soil through the preferred stream. Preferential flow plays an essential role in transferring metals from the soil profile. So that some of the metals added to the soil columns are absorbed into the environment. Some metals pass through the soil (Camobreco et al., 1996). Heavy metal cations (positive metal atoms) are also more mobile in acidic soil,

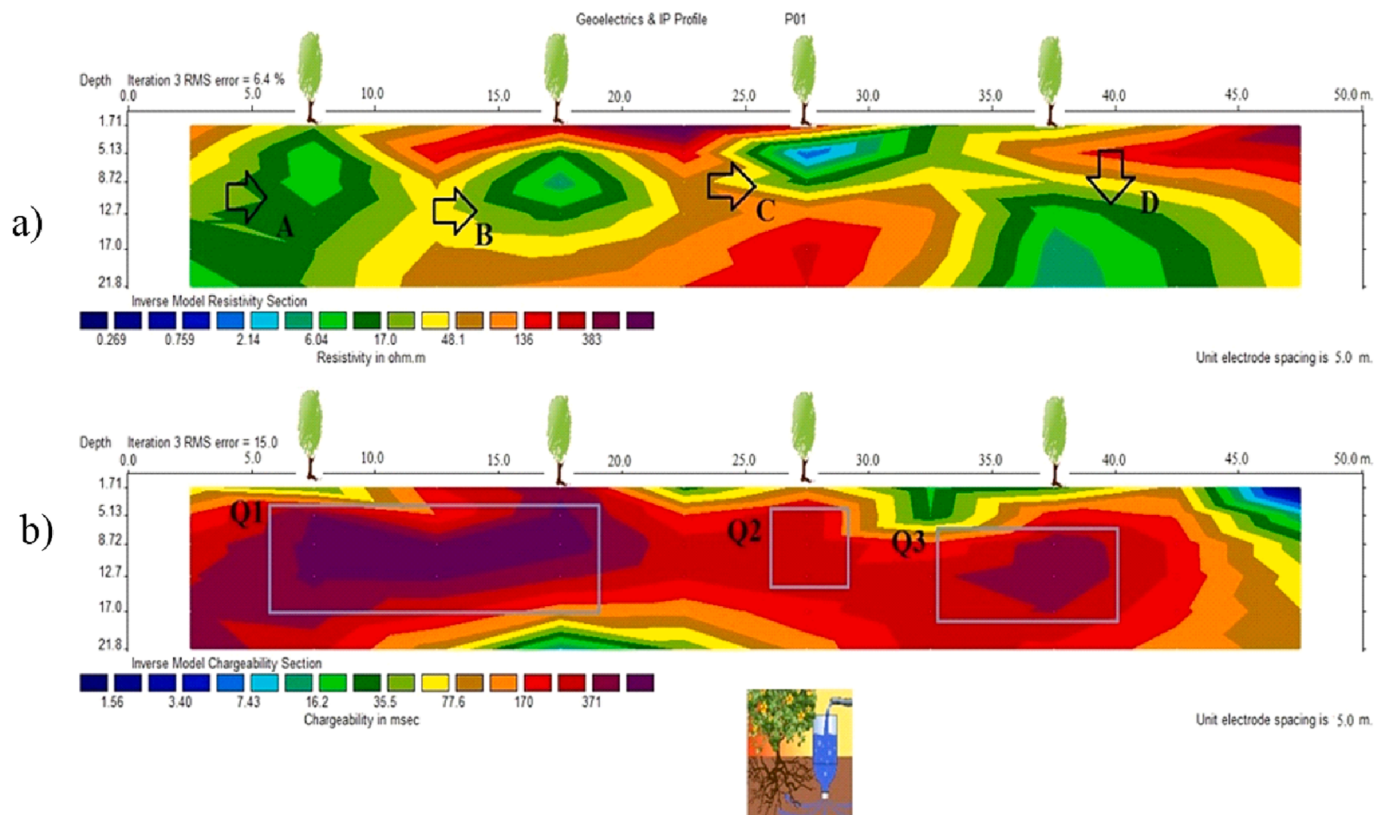


**Fig. 6.** Location of shrubs and priority areas in profile P01. a) Inverted resistivity model of profile 01, b) Inverted Induced polarization model of profile 01.

which means that metal pollutants are more readily available for plant uptake or transfer to a water source—of course, taking into account the role of factors such as surface potential, sorption capacity, point of zero charges, the impact of cation type.

The decrease in resistivity around the first shrub, which is about 7 m from the starting point of the profile, is quite pronounced because the mineral effluent's electrical conductivity due to the constituents is more than that of the surrounding soil studied region. As the supply areas are more affected by effluent infiltration, it increases over time. The movement of heavy metals in soil irrigated with effluent is very slow, so more than 90% of the cadmium, nickel and lead elements accumulate at a depth of 10–15 cm. Heavy metal accumulation at the irrigation site is attributed to the heavy metals' low dynamics and poor movement toward the lower layers. However, changes in the second shrub area at 17 m are not accompanied by a significant decrease in resistivity from the ground surface. This decrease is more than 5 m in depth. This range exists around the root of the plant. In the third shrub sub-area, 27 m from the starting point of the profile, the resistance has decreased from a depth of 2.5 m. So, the lateral effluent spread and pollution due to its location in the saturation zone is significant. In the third shrub sub-area, 27 m from the starting point of the profile, the resistance has decreased from a depth of 2.5 m. The lateral effluent spread and pollution due to its location in the saturation zone are significant. Due to the pool area (pool adjacent to the study area) and the possibility of waste materials around the fourth bush, the impermeable layer reduced the ground surface's resistivity. It was associated with a decrease in resistivity from more than 8 m deep. Also, the high composition of fine-grained soil may cause low permeability, thus having a higher capacity to retain more water to build high soil moisture content (Abidin et al., 2015). These changes are accompanied by an IP factor increase due to heavy metal accumulation in the induced polarization model. The addition is uniform at a distance of 2.5 and 21 m and shows a load (greater than 371 mV / s) from a depth of 4.16 to 18 m (red to purple). At a distance of 21 to 43 m, the charge is

170 to 371 mV/mS (red to dark red color), and at 34 to 39 m, the load increases at depths of 8 to 17 m (purple color).

The lead minerals salts are mostly chlorides. The affluent and chlorine leaching penetrate downstream. Parts A, B, C, and D increased electrical conductivity and water accumulation around the root. The salting soil damages the pores, and the air and water paths pass through the soil. Because salts must be in an ionic current to conduct, the amount of salt and mineral solutes in the soil determines the conduction paths. The electrical resistivity decreases with water increases (Samouelian et al., 2006). The semi-light (middle layer) and light (lower layer) textures are another reason for the heavy metal transfer. The movement of heavy metals in soils with large pores in the porous media can be due to the displacement of part of the colloidal sediments and clay particles. The heavy metals attached to these particles are also transported better (Alloway, 1990). Metals in soil with less organic matter move more quickly. In the lower model (Fig. 5), which is related to the induced polarization (IP) image, there was an increase in the induced polarization of the soil downstream, which is seen in zones Q1, Q2, and Q3, indicating an increase in the load ability in the downstream root zone. Increased load ability is detected when contamination with clay layers is due to ion exchange and heavy metal accumulation.

### 3.2. Two-dimensional model results of profile 2

After surveying Profile 02 (Fig. 6), resistivity and Induced polarization datasets were interpreted using RES2D&3D INV. Fig. 7a, b, and c show the measured apparent resistivity, calculated apparent resistivity, and inverse resistivity model.

#### 3.2.1. Investigation of resistivity and induced polarization of profile 2

Fig. 8 shows the trees' position and the geoelectrical resistivity levels two weeks after irrigation. Fig. 8a shows the 2D inverted model of the resistivity (by ohm/Ωm), and Fig. 8b shows the 2D inverse induced

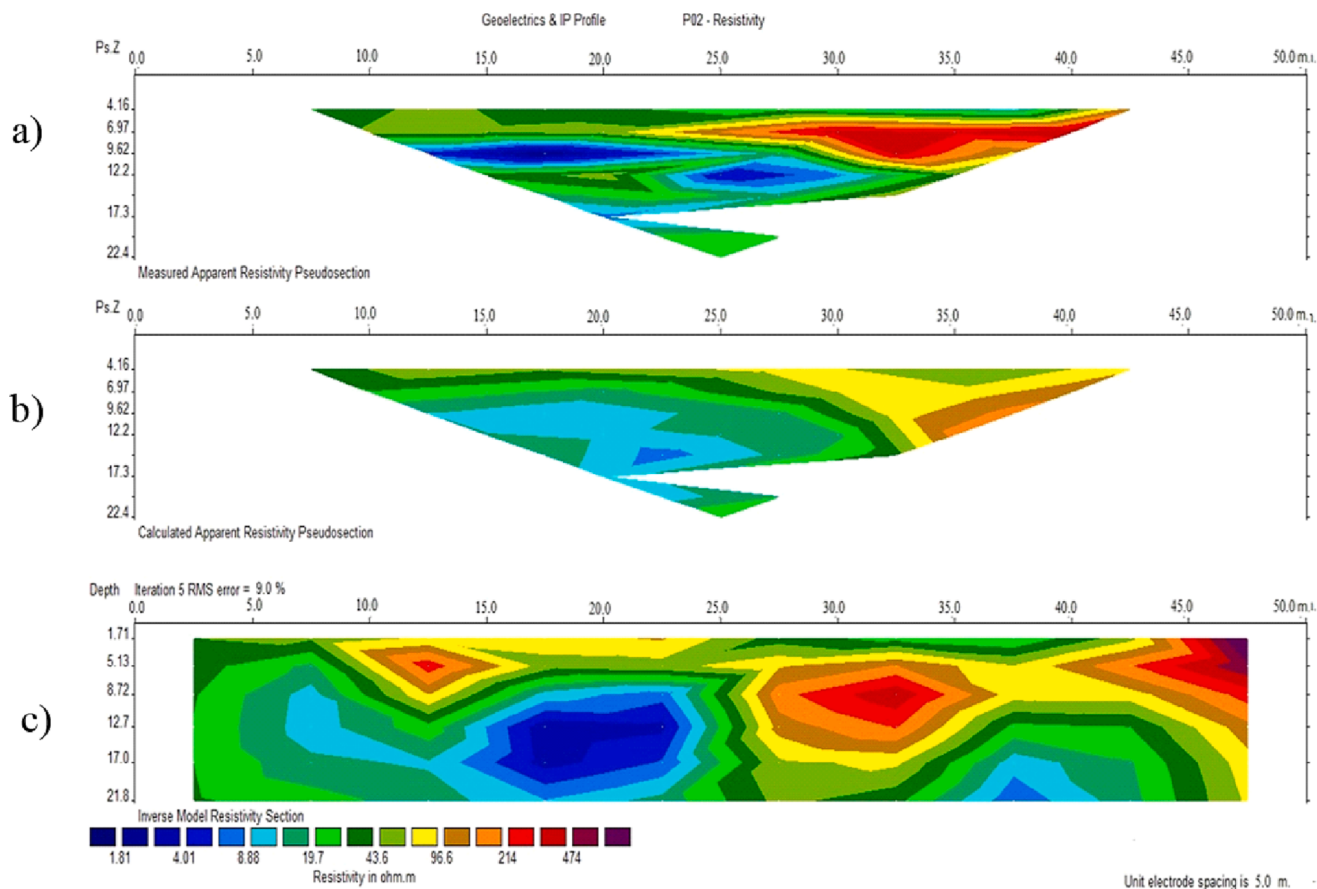


Fig. 7. a) Pseudo-section of measurements, b) pseudo-section of inversion, c) inverted resistivity model in profile P02 with 5 m electrode spacing.

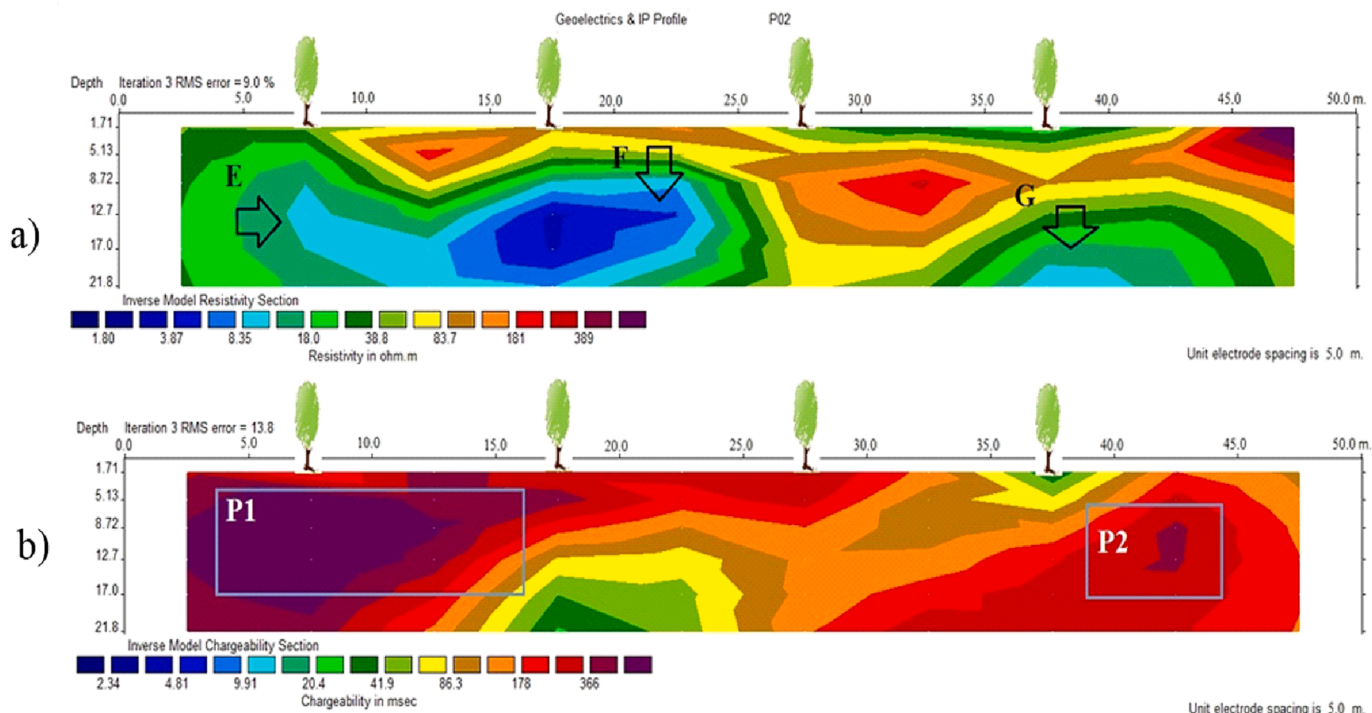
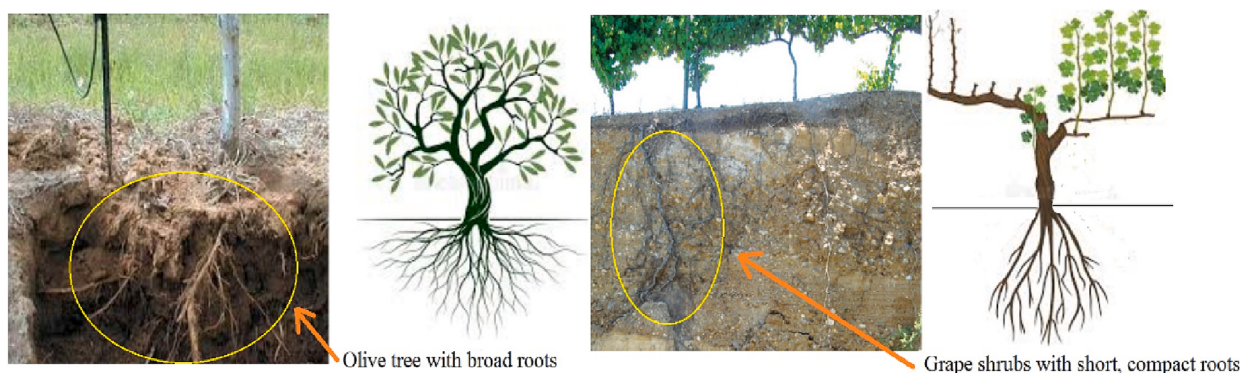
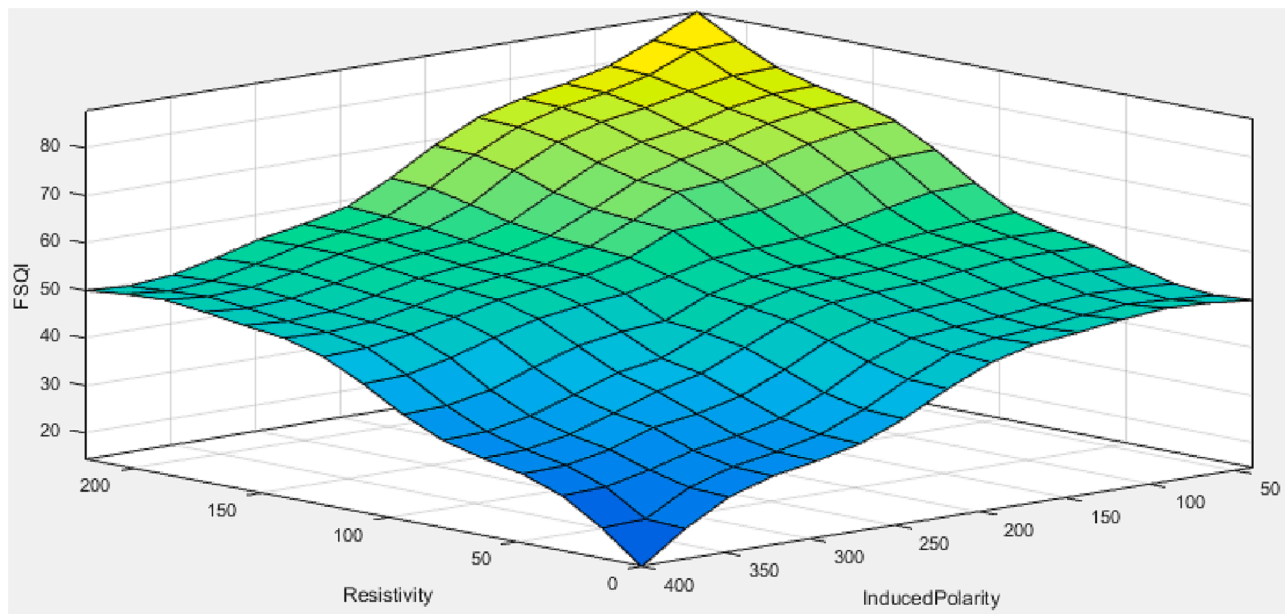


Fig. 8. Location of shrubs and priority areas in profile P02. a) Inverted resistivity model of profile 02, b) Inverted Induced polarization model of profile 02.



**Fig. 9.** The olive tree has broad roots, and grape shrubs have short and compact roots that make a different condition in absorbing pollutants from the soil.



**Fig. 10.** The output of FSQI vs. contamination factors in the fuzzy inference system.

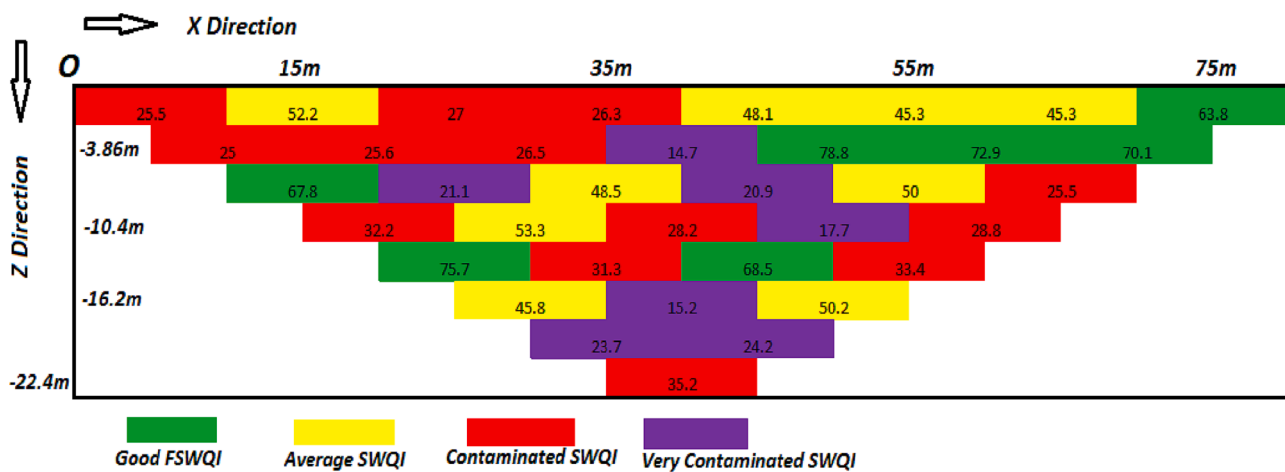


**Fig. 11.** FSQI mapping in Profile P01.

polarization model (in millivolts per millisecond). The decrease in vertical resistivity around the first and second trees shows a lower depth since the beginning of irrigation, and these areas have been steadily

laterally expanding. There is a decrease in resistivity at the third shrub/tree's surface. The expansion is not vertical but lateral and directed to the fourth tree's lower area.

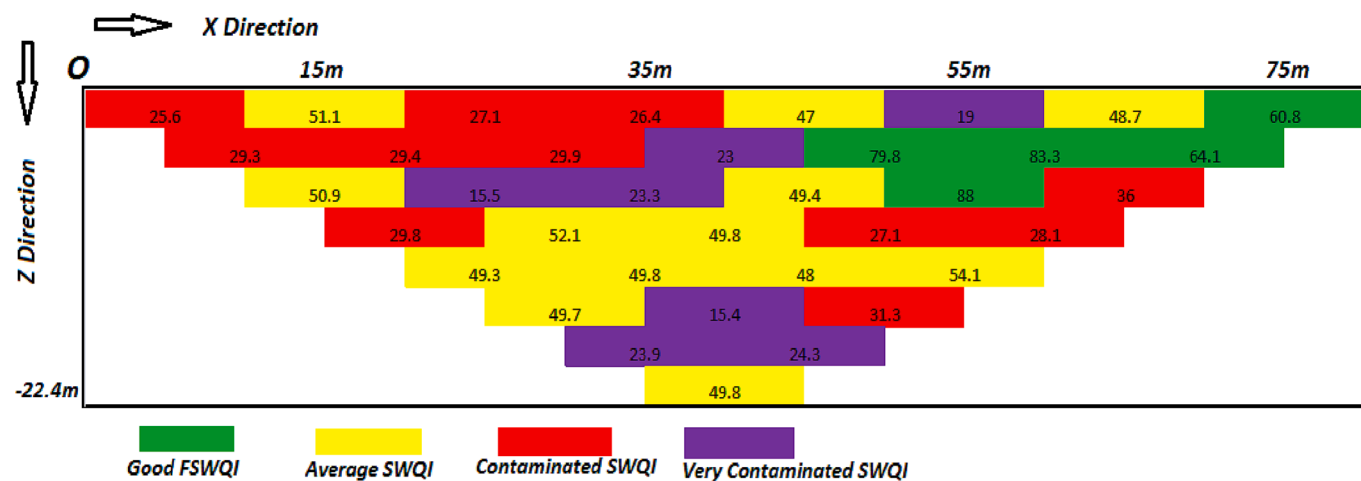


Fig. 12. FSQI mapping in Profile P02.

Table 3

Averages of FSQI of rows and columns in Two-D mapping in Profile P01.

Columns Rows	5 m	15 m	25 m	35 m	45 m	55 m	65 m	75 m
Average Of Columns FSQI	25.25	40.56	38.4	31.7	36.5	47.1	48.5	66.9
Average Of Rows FSQI								
-0.077 m	41.68							
-3.86 m	44.8							
-6.95 m	38.96							
-10.04 m	32.04							
-13.13 m	52.22							
-16.22 m	37.06							
-19.3 m	23.95							
-22.4 m	35.2							

Table 4

Averages of FSQI of rows and columns in Two-D mapping in Profile P02.

Columns Rows	5 m	15 m	25 m	35 m	45 m	55 m	65 m	75 m
Average Of Columns FSQI	27.45	38.1	35.35	35.73	40.4	51.33	52.04	62.45
Average Of Rows FSQI								
-0.077 m	38.21							
-3.86 m	48.4							
-6.95 m	43.85							
-10.04 m	37.38							
-13.13 m	50.3							
-16.22 m	32.13							
-19.3 m	24.1							
-22.4 m	49.8							

The decrease in the resistivity in the mid to the bottom of this profile can be attributed to the presence and lateral spread of the contamination over time with increasing depth or moisture content of the soil and fine-grained sediments. The decrease in the resistivity indicates the severity of the contamination and its spread east and south of the surveyed zone. In the induced polarization model, these changes are relatively uniform and associated with increased chargeability properties. Furthermore, the root zone's resistivity increases to a depth of 8 m, and the downstream regions E, F, and G are shown in the resistivity model. This increase in resistivity under the bushes can be attributed to soil drying or dissolved ions by the plant root. The insoluble lead salts are readily absorbed by the sprout and surface roots of the bushes and shrubs. Many biological process reducers and oxidizers create spaces in this layer that reduce or alter biological contamination in the soil's root zone. The lateral depth and breadth of the roots affected pollution concentration in the soil. The passage of effluent through the unsaturated area of the earth (between

groundwater and soil surface) allows the separation of floating solid particles, decomposable materials, and microorganisms. Usually, it reduces the concentration of pollutants (Hosseinpour et al., 2009). Due to the absorption of more water and solutes, the vegetation, especially at the peak of growth stages, significantly reduces the amount of water entering the earth's strata in the washing process and leaking (Zvomuya et al., 2005; Basso and Ritchie, 2006). After absorption, the lead is readily transported in the plant, and this transition depends mainly on the plant's physiological state. According to the study (Arani et al., 2016), as the lead uptake concentration was increased in the roots, the lead concentration was less than 200 mg/L. The olive plant was able to counteract the toxicity of lead. Furthermore, in this study, the amounts of lead that can damage plants are listed differently (Fig. 9).

In the induced polarization model, the range of induced polarization can be seen as smaller than the P01 profile. Areas with high IP are smaller than other parts. This high IP value may be because lead and

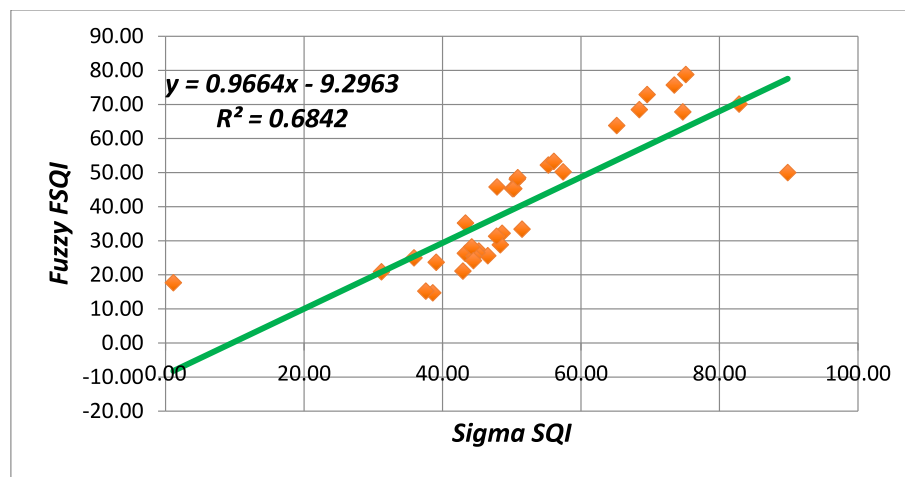


**Fig. 13.** Linear regression validation of fuzzy SQI vs. SigmaSQI in Profile P01.

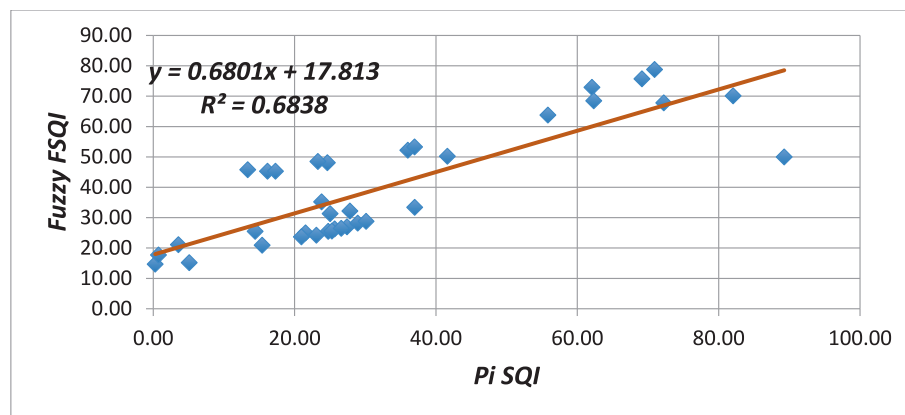


**Fig. 14.** Linear regression validation of fuzzy SQI vs. PiSQI in Profile P01.

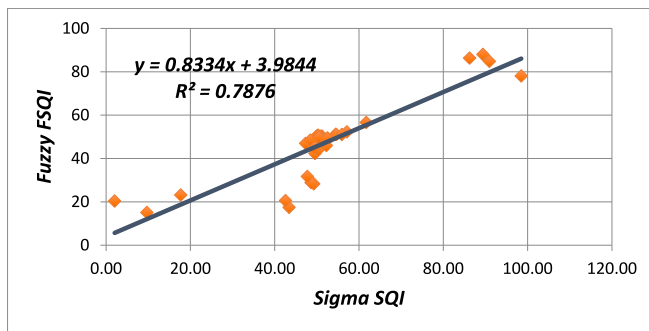


**Fig. 15.** Linear regression validation of fuzzy SQI vs. SigmaSQI in Profile P02.

copper usually form strong bonds with organic matter and are released slowly due to the low decomposition rate of organic matter. Lead and zinc form a weaker bond with organic matter. Also, clay minerals can remove heavy metal ions from aqueous solutions because of their unique properties, such as high specific surface area, high cation exchange capacity, and strong adsorption ability. Adsorption or desorption of heavy metals in soil is controlled by various factors such as pH, soil type and quality, concentration, and competing ions to absorb organic matter content, clay minerals, calcium carbonate, iron-manganese oxides, ionic strength, and soil particle size change (Achiba et al., 2009).

The resistivity and induced polarization models show that contamination is present in both profiles; in-depth sampling and analysis

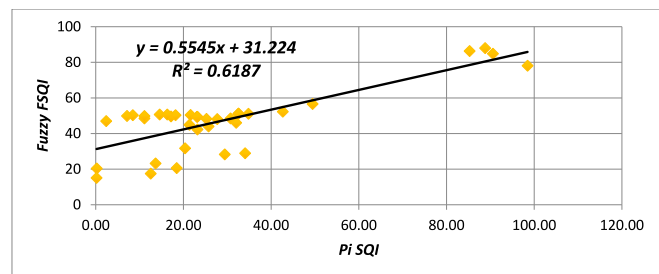


**Fig. 16.** Linear regression validation of fuzzy SQI vs. PiSQI in Profile P02.

confirm this point. So, this contamination is indicated by decreasing the resistivity and increasing induced polarization. Moreover, it can determine the uptake rate of contaminants by the root system of trees and shrubs.

### 3.3. FSQI, SigmaSQI and PiSQI

**Fig. 10** illustrates the output of fuzzy resounding for mapping FSQI Vs. contamination factors: Induced Polarization and Resistivity. As shown, resistivity is direct while the effect of IP is reversed, which means increasing resistivity increases the SQI because it exhibits fewer values for contamination concentration. In contrast, increasing induced polarization decreases the SQI because it represents more contamination in the studied area.

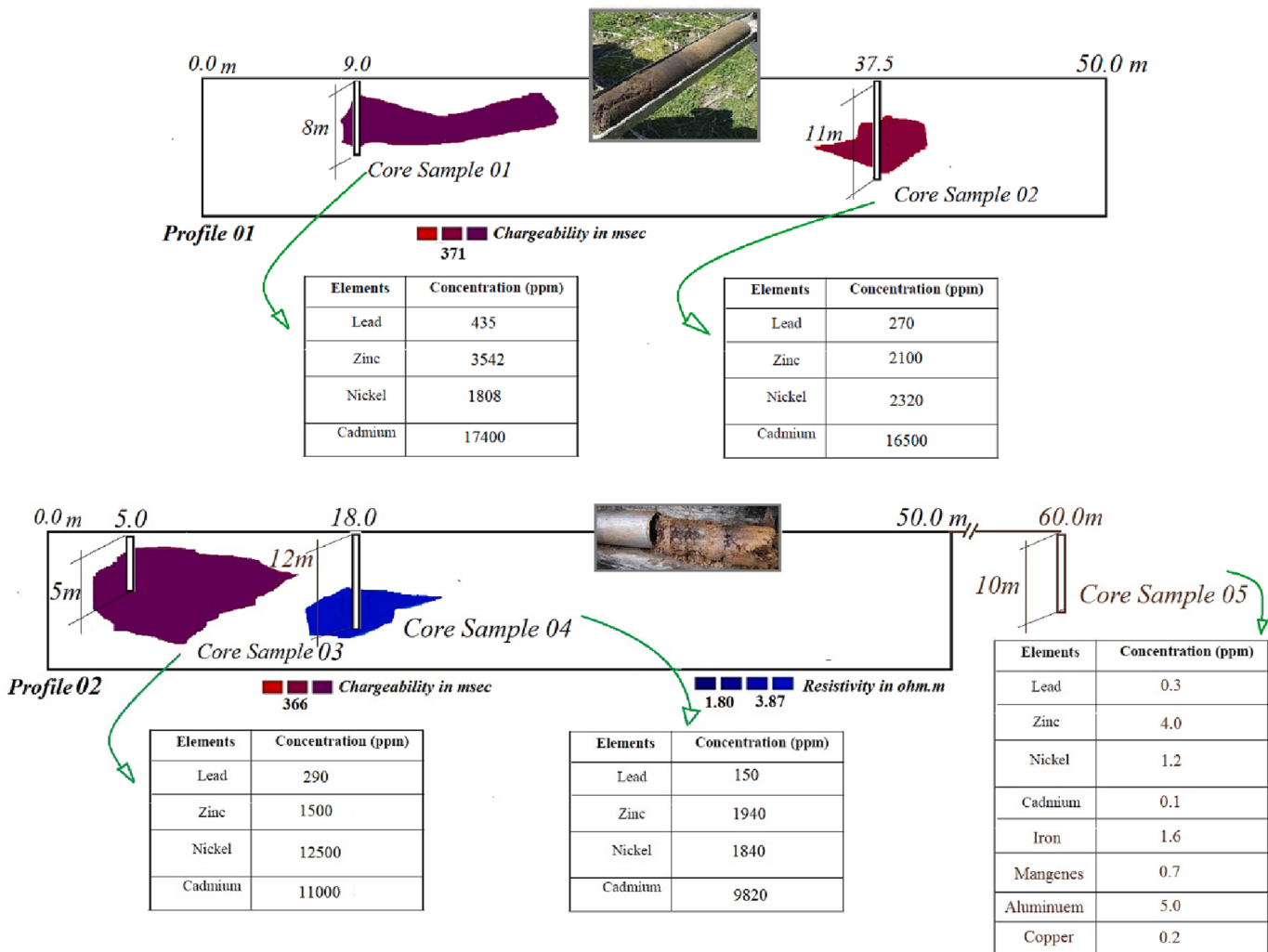


**Fig. 17.** Five soil samples with different depths on geophysical profiles No. 1 and 2, along with the results of some heavy metals, were analyzed for validation.

The results of two-dimensional mapping for the fuzzy soil quality index are depicted in Fig. 11 for profile P01 and Fig. 12 for profile P02.

The results for averages of FSQIs of rows and columns of two-dimensional mapping for study profiles can be studied via Table 3 and Table 4.

As extracted from Tables 3 and 4, the maximum average column FSQIs occurs in column 75 m by 66.9 for Profile P01 and 62.45 for Profile P02. On the other hand, the minimum average FSQIs occur in column 5 m by the amount of 25.25 for Profile P01 and 27.45 for Profile P02, which is mainly due to the slope of the watering line bringing about more concentration of contaminants in this column (Keep this in mind that low amounts of FSQI represent low degrees of cleanliness and quality). Besides, the maximum average of Row FSQIs occurs in -13.13 m for both Profiles. The Row -13.13 m of Profile P01 has FSQI equal to 52.22, and this amount for Profile P02 is 50.3. On the other hand, the minimum average of Row FSQIs occurs in -19.3 m for both Profiles. For profile P01, the minimum FSQI equals 23.95, while this amount equals 24.1 for Profile P02. Z-direction variations of FSQI reveal the role of planting. In the case of no planted trees, the Row -0.077 m FSQI had higher values than Row -3.86 m, and the decreasing pattern existed from row 1 to row 4 or even to row 8. However, in the case of planted trees as Profile p01, the decreasing pattern contravenes, and the Row -0.077 m receives FSQI about, 41 which is smaller than that of the Row -3.86 m is about 44 (41 less than 44). For Profile P02, the decreasing pattern fails, and the Row -0.077 m receives FSQI of about 38, which is smaller than that of the Row -3.86 m is about 48 (38 less than 48). This

happens because the trees' roots adsorb the contaminants near the ground surface, which brings about higher concentrations of contaminants than in deeper layers. This phenomenon is understood in Figs. 11 and 12 too. The highest fuzzy soil quality indices in both figures are present in columns 45 m to 75 m and the Row of -3.86. The effect of this study is more by analyzing older trees with more extended and broader roots. The planted trees play a very influential role in decreasing contaminants and enhancing soil quality indices.

The results of cross-validations are illustrated in Figs. 13 to 16. Respectively, Fig. 13 demonstrates the cross-validation for fuzzy SQI vs. SigmaSQI, and Fig. 14 illustrates the linear validation of fuzzy SQI vs. PiSQI in Profile P01. The corresponding R square parameter is about 0.68 for FSQI vs. SigmaSQI and PiSQI, which exhibit an even distribution of fuzzy indices concerning statistical indices in Profile P01. Fig. 15 illustrates the validation of FSQI vs. SigmaSQI, and Fig. 16 demonstrates the validation for FSQI vs. PiSQI in Profile P02. The respective R square parameter is about 0.78 for FSQI vs. SigmaSQI and is about 0.62 for FSQI vs. PiSQI in Profile P02.

Altogether it is derived from data that the fuzzy notion is closer to aggregative weighted SQI.

#### 4. Validation

In the following, for validating these general and special FSQI research models and summarizing the results, five soil profile samples with depths of 8, 11, 5, 12, and 10 m (so that the geophysical parameters

Res/IP and FSQ Index with changes in geophysical and fuzzy SQI parameters can be directly observed and analyzed), according to Fig. 17 was collected using a soil sample from the cores particles, which was used to analyze the components and amount of pollutants related to irrigation with wastewater (especially, lead, zinc, nickel, and cadmium). The samples were analyzed at critical points/depths, and the results presented/tables showed good compliance with the introduced methods. One of the essential cases of research at this stage is "core sample 05", which was taken at a distance of 10 m from the end of the geophysical surveyed profile and analyzed, which shows that the amount of heavy metals in the natural soil of the study area is minimal. Furthermore, it can be mentioned that the background amounts of heavy metals do not affect the research results.

## 5. Conclusion

Soil contamination is a challenge for the environment, spreading due to the development of industries and mines. Thus, pollutants related to industrial and mining activities can negatively affect the agronomic characteristics and productivity of surface soils and groundwater resources. Geophysical methods, such as the geoelectric method with this study's design, can effectively investigate the extent of soil contamination with contaminants from leakage and infiltration of drained water of lead and zinc mines in its subsurface. According to the existing soil profile from the study area (College of Environment), except for the 20 cm surface layer above the earth, which was removed from around the electrodes during geophysical data collection. Up to 25 m from the earth's surface, no significant changes have been observed in the soil type, texture, and granularity. Also, the water table level in this area is about 150 m in depth, so the changes in resistance are solely dependent on the changes in the amount of lead and zinc wastewater pollution. This research first designs irrigation experiments using wastewater effluent of lead and zinc mines in the Zanjan region. Furthermore, changes in these contamination anomaly ranges have been identified due to simultaneous resistivity data and induced polarization surveying in time-lapse and investigating the spread of pollution in this region's subsoil. So, geophysical models result in a time-lapse surveyed profile that can identify the extent of contamination of the lead and zinc wastewater and determine its spreading and absorbing location in the plant's root zone (olive and grape bushes roots) be seen in Fig. 9. This method can also provide appropriate solutions to reduce pollution to avoid the high cost of cleaning up contaminated areas to apply for polluted regions near the lead and zinc drainage of the Anguran mine in Zanjan. The results show that the plants with the broad root system (olive tree used in this experiment) absorb contaminants from the soil, reducing the risk of leaching and penetrating heavy metal (lead and zinc) contaminants into the subsoil and aquifer. Detecting and modeling the contamination plume by identifying the polluted area through rapid and cost-effective geophysical methods is also advisable. Also, five validation soil samples were analyzed in critical sections; furthermore, the results presented by the introduced methods showed suitable compliance.

## CRediT authorship contribution statement

**Hamid Sarkheil:** Project administration, Conceptualization, Supervision, Writing – review & editing. **Khadijeh Sadoughi Noughabi:** Writing – review & editing, Investigation. **Yousef Azimi:** Writing – review & editing. **Shahrokh Rahbari:** Resources.

## Declaration of Competing Interest

The authors declare that they have no known competing financial interests or personal relationships that could have appeared to influence the work reported in this paper.

## Data availability

Data will be made available on request.

## Acknowledgment

The authors thank the College of Environment, Department of Environment (DOE) authorities for their support. The authors declare that there is no conflict of interest.

## Appendix A. Supplementary data

Supplementary data to this article can be found online at <https://doi.org/10.1016/j.ecolind.2023.110362>.

## References

- Abidin, M.H.Z., Saad R., Wijeyesekera, D.C., Ahmad, F., Tajudin, S.A., Madun, A., Bakar, I., 2015. Soil Identification Using Field Electrical Resistivity Method. *J. Phys.: Conference Series* 495. IOP Publishing.
- Achiba, W.B., Gabteni, N., Lakhdar, A., Laing, G.D., Verloo, M., Jedidi, N., Gallali, T., 2009. Effects of a 5-year municipal solid waste compost application on heavy metals' distribution and mobility in a Tunisian calcareous soil. *Agr. Ecosyst. Environ.* 130, 156–163.
- Akowuah, E., 2011. Computational Modeling of the Movement of Water Soluble Pollutants in the Soil.
- Alloway, B.J., 1990. *Heavy Metal in Soil*. Blackie and Son Ltd., London, p. 339p.
- Arani, M., Khosravi, A., Azimzadeh, M., Sudaiizadeh, H., 2016. Investigation of Lead and Cadmium Accumulation and Some Physiological Responses in Olive Species for Use in Phytoremediation. *J. Plant Ecophysiol.*, Eighth Year, No. 26-pp 204-195.
- Ariafar, A., Mohammad Qasemi, T., Ghorbani, A., 2014. Geophysical and Environmental Geochemical Study to Investigate the Pollution Effects of Qale Zari Copper Mine Wastewater, South Khorasan. *J. Min. Eng.* 9 (23), 81–94.
- Camobreco, V.J., Richards, B.K., Steenhuis, T.S., Peverly, J.H., McBride, M.B., 1996. Movement of heavy metals through undisturbed and homogenized soil columns. *Soil Sci.* 161 (11), 740–750.
- Campbell, D.L., Fitterman, D.V., 2000. *Geoelectrical Methods for Investigating Mine Dumps*. Organization: Society for Mining, Metallurgy & Exploration, Pag: 12.
- Dijkstra, F., 1998. A micromorphological study on the development of humus profiles in heavy metal polluted and nonpolluted soils under Scots pine. *Geoderma* 82, 341.
- Gillet, S., Ponge, J.F., 2002. Humus forms and metal pollution in the soil. *European. J. Soil Science* 53, 529.
- Hosseinpour, A., Haghnia, G., Alizadeh, A., Fotut, A., 2009. Investigation of Chemical Quality Changes in Raw Wastewater and Urban Wastewater by Crossing Soil Columns. *J. Water Soil* 22 (3), 45–56.
- Huang, Y., Wang, L., Wang, W., Li, T., He, Z., Yang, X., 2019. Current status of agricultural soil pollution by heavy metals in China: A meta-analysis. *Sci. Total Environ.* 651, 3034–3042.
- Jelenska, M., Hasso-Agopsowicz, A., Kadzialko-Hofmokl, M., Kopcewicz, B., Sukhorada, A., Bondar, K., Matviishina, Z., 2008. Magnetic Structure of Polluted Soil Profiles from eastern Ukraine. *Acta Geophys.* 2008 (56), 1043–1064.
- Kabata Pendias, A., 2010. *Trace Elements in Soils and Plants*. CRC Press, Boca Raton., New York, p. 400p.
- Knodel, K., Krummel, H., Lange, G., 2005. *Handbook for exploring the subsoil of landfills and contaminated sites*. Springer, Berlin, Heidelberg, p. 2005.
- Koda, E., 2012. Influence of Vertical Barrier Surrounding Old Sanitary Landfill on Eliminating Transport of Pollutants based on Numerical Modeling and Monitoring Results. *Pol. J. Environ. Stud.* 2012 (21), 929–935.
- Kuras, O., Wilkinson, P.B., Meldrum, P.I., Oxby, L.S., Uhlemann, S., Chambers, J.E., Binley, A., Graham, J., Smith, N.T., Atherton, N., 2016. Geoelectrical monitoring of simulated subsurface leakage to support high-hazard nuclear decommissioning at the Sellafield Site, UK. *Sci. Total Environ.* 566-567, 350–359.
- Loke, M.H., Chambers, J.E., Rucker, D.F., Kura, O., Wilkinson, P.B., 2013. Recent Developments in the Direct-Current Geoelectrical Imaging Method. *J. Appl. Geophys.* 95, 135–158.
- Maas, S., Scheifler, R., Benslama, M., Crini, N., Lucot, E., Brahmia, Z., Benyacoub, S., Giraudoux, P., 2010. Spatial distribution of heavy metal concentrations in urban, suburban, and agricultural soils in a Mediterranean city of Algeria. *Environ. Pollution.* 158 (6), 2294–2301.
- Magiera, T., Źogala, B., Szuszkiewicz, M., Pierwola, J., Szuszkiewicz, M.M., 2019. Combination of different geophysical techniques for the location of historical waste in the Izery Mountains (SW Poland). *Sci. Total Environ.* 682, 226–238.
- Maleki, A., Hashmati Moghadam, M., 2014. Mines and tailings mines and environmental impacts, Second National Conference on Zagros Environmental Hazards - Tehran, March 2014.
- Masmoudi Charfi, C., Masmoudi, M., Ben Mechlia, N., 2011. Root distribution in young "Chéroui" olive trees and agronomic applications. *Adv. Hortic. Sci.* 25 (2), 112–122.
- Mazej, Z., Al Sayegh-Petkovsek, S., Pokorný, B., 2010. Heavy metal concentrations in the food chain of Lake Velenjsko jezero, Slovenia: an artificial lake from mining. *Arch. Environ. Contam. Toxicol.* 58, 998–1007.

- Moradzadeh, A., Ardejani, F.D., Shokri, B.J., Sarkheil, H., Osanloo, M., 2007. A method for coal waste disposal site selection for prevention of environmental impacts, IMWA Symp. 2007: Water in Mining Environments, Italy, 239–243.
- Samouelian, A., Cousin, I., Tabbagh, A., Bruand, A., Richard, G. 2006. Electrical resistivity survey in soil science: a review, *Soil and Tillage Research*, Elsevier, 83, pp.2: 173- 193.
- Sarkheil, H., Habibi Rad, M., 2015. 4D Electrical Resistivity Tomography Monitoring of Talesh Mahaleh-Rasht Coastal Aquifer Polluted by Caspian Seawater, Conference Proceedings, Near Surface Geoscience 2015 - 21st European Meeting of Environmental and Engineering Geophysics, Sep 2015, Volume 2015, p.1 – 5. 10.3997/2214-4609.201413795.
- Sarkheil, H., Hassani, H., 2009. A new design for geoelectric surveying and inverse 1D and 2D modeling: the case of Karongah lead-zinc mine, 9th International Multidisciplinary Scientific GeoConference (SGEM), Bulgaria.
- Sarkheil, H., Azimi, Y., Rahbari, S., 2018. Fuzzy wastewater quality index determination for environmental quality assessment under uncertain and vagueness conditions. *Int. J. Eng. Transact. B*. 31 (8), 1196–1204.
- Sarkheil, H., Azimi, Y., Rahbari, S., 2019. Fuzzy Wastewater Quality Index (FWWQI) for Environmental Quality Assessment of Industrial Wastewater, a Case Study for South Pars Special Economic and Energy Zone. *J. Civil Environ. Eng.* pp. <https://doi.org/10.22034/jcee.2019.9101>.
- Sarkheil, H., Vaseghi, B., Ziarati, K., 2014. Analysis of discontinuities and ground waters in the SHORGOL-SALMAS quarry stone mine using geophysical methods, Conference Proceedings, 6th EAGE Saint Petersburg International Conference and Exhibition, Apr 2014, Volume 2014, p.1 – 5. doi:10.3997/2214-4609.20140298.
- Sarkheil, H., Rahbari, S., 2016. Development of case historical, logical air quality indices via fuzzy mathematics (Mamdani and Takagi-Sugeno systems), a case study for Shahre Rey Town. *Environ. Earth Sci.* 75, 1319. <https://doi.org/10.1007/s12665-016-6131-2>.
- Sarkheil, H., Azimi, Y., Rahbari, S., 2018a. Modeling environmental air quality assessment using fuzzy logic in the Pars Special Economic Energy Zone (Case study: Assaluyeh, Bidkhon and Shirino regions). *J. Environ. Sci. Technol.* 20 (4), 1–16. <https://doi.org/10.22034/jest.2019.13698>.
- Sarkheil, H., Azimi, Y., Rahbari, S., 2018b. Fuzzy Wastewater Quality Index Determination for Environmental Quality Assessment under Uncertain and Vagueness Conditions'. *Int. J. Eng.* 31 (8), 1196–1204.
- Sarkheil, H., Tahery, B., Rayegani, B., Ramezani, J., Goshtasb, H., Jahani, A., 2020. Evaluating the current status of the national health, safety, and environment management system for integration, harmonization, and standardization of environmental protection. *Health Risk Analysis* 18–24.
- Sarkheil, H., Rahbari, S., Azimi, Y., 2021. Fuzzy-Mamdani environmental quality assessment of gas refinery chemical wastewater in the Pars special economic and energy zone. *Environ. Challenges* 3, 100065.
- Sharafi, A., Sarkheil, H., Hafizi, M.K., 2014. Inverse Least-Squares Modeling of Induced Polarization and Resistivity Data to Explore Copper Deposits in the Sarbisheh Ophiolites, Iran. *Int. J. Emerg. Sci. Eng. (IJESE)*. ISSN: 2319-6378, Volume-2 Issue-12.
- Singh, J., Kalamdhad, A., 2011. Effects of Heavy Metals on Soil Plants, Human Health, and Aquatic Life. *Int. J. Res. Chem. Environ.* 1 (2011), 15–21.
- Smart, D.R., Schwass, E., Lakso, A., Morano, L., 2006. Grapevine Rooting Patterns: A Comprehensive Analysis and a Review. *Am. J. Enol. Vitic.* 57 (1), 89–104.
- Sparrenbom Charlotte, J., Akesson, S., Johansson, S., Hagerberg, D., Dahlén, T., 2017. Investigation of chlorinated solvent pollution with resistivity and induced polarization. *Sci. Total Environ.* 575, 767–778.
- Zeng, S., Ma, J., Yang, Y., Zhang, S., Liu, G.-J., Chen, F.u., 2019. Spatial assessment of farmland soil pollution and its potential human health risks in China. *Sci. Total Environ.* 687, 642–653.
- Zvomuya, F., Gupta, S.C., Rosen, C.J., 2005. Phosphorus Leaching in Sandy Outwash Soils following Potato-Processing wastewater application. *J. Environ. Qual.* 34 (4), 1277–1285.
- Telford, W.M., Geldart, L.P., Sheriff, R.E., 1990. *Applied Geophysics*. London: Cambridge University Press, 522 - 577.
- Kemna, A., 2012. An overview of the spectral induced polarization method for near-surface applications. Lawrence Berkeley National Laboratory. doi:DOI: 10.3997/1873-0604.2012027.
- Sarkheil, H. Shirkhani, D., Azimi, Y., Talebi, A., Rahbari, S., 2023. Fuzzy radon hazard index assessment for stochastic environmental health risk evaluation of urban scale building Stoch. *Environ. Res. Risk. Assess.* doi:10.1007/s00477-023-02460-x.